BIOCHEMISTRY
including biophysical chemistry & molecular biology

Article

pubs.acs.org/biochemistry

High-Resolution HPLC–ESI–MS Characterization of the Contact Sites of the Actin–Thymosin β_4 Complex by Chemical and Enzymatic Cross-Linking

Jana Knop,*[,†] Christine App,[†] Anselm H. C. Horn,[†] Federica Iavarone,[‡] Massimo Castagnola,[‡,§] and Ewald Hannappel[†]

[†]Institut für Biochemie, Emil-Fischer-Zentrum, Friedrich-Alexander-Universität Erlangen-Nürnberg, 91054 Erlangen, Germany

[‡]Istituto di Biochimica e Biochimica Clinica, Facoltà di Medicina, Università Cattolica, 00168 Roma, Italy

[§]Istituto per la Chimica del Riconoscimento Molecolare, Consiglio Nazionale delle Ricerche, 00185 Roma, Italy

ABSTRACT: Thymosin β_4 sequesters actin by formation of a 1:1 complex. This transient binding in the complex was stabilized by formation of covalent bonds using the cross-linking agents 1-ethyl-3-(3-dimethylaminopropyl)carbodiimide and a microbial transglutaminase. The localization of cross-linking sites was determined after separating the products using SDS-PAGE by tryptic in-gel digestion and high-resolution HPLC–ESI–MS. Three cross-linked fragments were identified after chemical cross-linking, indicating three contact sites. Because the cross-linked fragments were detected simultaneously with the corresponding non-cross-linked fragments, the three contact sites were not formed in parallel. K3 of thymosin β_4 was cross-linked to E167 of actin, K18 or K19 of thymosin β_4 to one of the first three amino acids of actin (DDE), and S43 of thymosin β_4 to H40 of actin. The imidazole ring of histidine was proven to be an acyl acceptor for carbodiimide-mediated cross-linking. Molecular modeling proved an extended conformation of thymosin β_4 along the subdomains 1 to 3 of actin. The enzymatic cross-linking using a microbial transglutaminase led to the formation of three cross-linking sites. Q41 of actin was cross-linked to K19 of thymosin β_4, and K61 of actin to Q39 of thymosin β_4. The third cross-linking site was identified between Q41 of actin and Q39 of thymosin β_4, which are simultaneously cross-linked to K16, K18, or K19 of thymosin β_4. When both cross-linking reactions are taken together, the complex formation of actin by thymosin β_4 is more likely to be flexible than rigid and is localized along the subdomains 1 to 3 of actin.

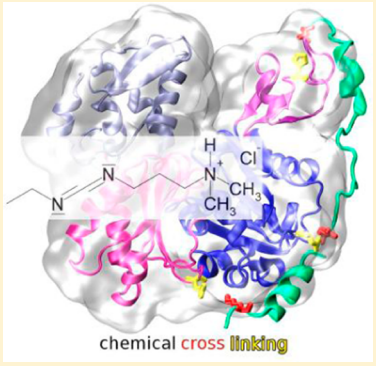

INDRODUCTION

Thymosin β_4 (Tβ_4) is a multifunctional, 5 kDa peptide containing 43 amino acids. It is present in almost every type of cell and tissue with the exception of erythrocytes.[1] It is a member of the highly conserved peptide family of β-thymosins, which exist in vertebrates and invertebrates.[2] In 1991, Safer et al. identified Tβ_4 as a G-actin sequestering peptide. Tβ_4 forms a 1:1 complex with monomeric G-actin and inhibits the polymerization to F-actin. The K_d for the actin–Tβ_4 complex is dependent on the bound nucleotide at the central nucleotide binding site of G-actin and is 0.5–2.5 μM in ATP and 50 μM in ADP.[3]

Actin, a structural protein, is present in all eukaryotic cells and is an essential part of the cytoskeleton. The cytoskeleton is responsible for mechanic stability and cell shape as well as intracellular transport processes and locomotion.[4] A prerequisite for these functions is the dynamic process of de- and repolymerization of actin.[5] Tβ_4 is known to inhibit the polymerization of monomeric actin by a steric mechanism so that the critical concentration of monomeric actin, necessary for polymerization, is not reached.[6]

The actin–Tβ_4 complex is very unstable, and crystallization of the complex to determine the structure has not yet been accomplished. Irobi et al. were able to crystallize a complex of actin and a Tβ_4 chimera.[7] Thereby, the binding of the Tβ_4 fragment (21–43) to actin may be influenced by the attached gelsolin fragment (27–152), which is an actin binding protein itself. Also classical nuclear magnetic resonance (NMR) methods to define the actin–Tβ_4 complex are problematic because of the small size of Tβ_4, low stability, and large size of the complex, as well as technical difficulties.[8] However, Domanski et al. proposed a structure of Tβ_4 bound to G-actin using NMR and predicted a N-terminal α-helix (residues 6–13) and a C-terminal α-helix (residues 31–40).[8]

Previous studies on the identification of contact sites in the actin–Tβ_4 complex used highly elaborate and sophisticated methods, such as sequential proteolytic digestion with HPLC and amino acid analyses or distance-dependent thiol cross-linking with different mutants of Tβ_4.[9] Both studies identified the contact site between subdomain 1 of actin and the N-terminal region of Tβ_4. However, the central part of Tβ_4 was bound to the N-terminus of actin in subdomain 1 according to

Received: May 28, 2013
Revised: July 24, 2013
Published: July 26, 2013

   dx.doi.org/10.1021/bi400664k | *Biochemistry* 2013, 52, 5553–5562

Safer et al.,[9a] whereas Reichert et al.[9b] identified the ATP analogue as the binding partner (Figure 1). The present study

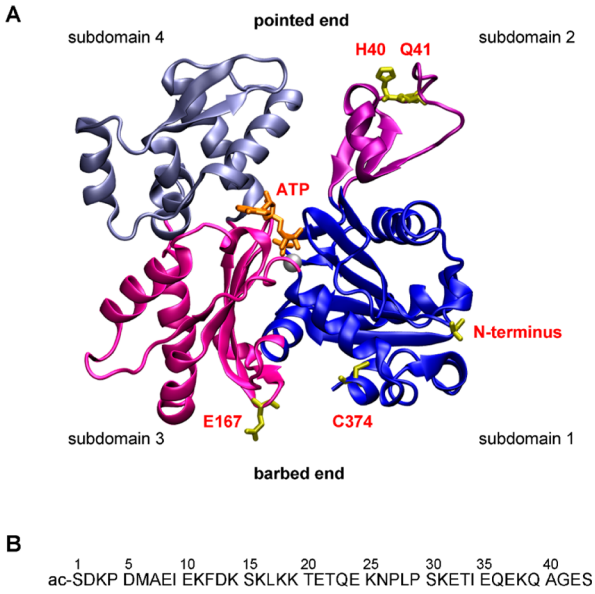

Figure 1. Actin and Tβ_4. (A) Actin divided in four subdomains, as indicated by different colors in the model. The published contact sites of Tβ_4 within the actin molecule are labeled in red. Safer et al. identified amino acids 1–4 and E167 by chemical, as well as Q41 by enzymatic, cross-linking.[9a] Reichert et al. postulated the binding at C374 and the central ATP.[9b] De la Cruz et al. were able to cross-link Tβ_4 to H40 of actin.[35] (B) Amino acid sequence of Tβ_4 (Uniprotkb: P62328), the N-terminus is acetylated.

tried to shed more light on the complex binding situation of Tβ_4 and actin and locates contact sites in the actin–Tβ_4 complex in detail using high-performance liquid chromatography (HPLC) combined with electrospray ionization (ESI) and high-resolution mass spectrometry (MS) on the trypsin digests of the covalently bonded complex from chemical and enzymatic cross-linking reactions.

MATERIALS AND METHODS

Proteins. G-actin was isolated from bovine heart muscle by the method of Pardee and Spudich[10] and stored at 0 °C in buffer (2 mM Tris/HCl pH 8.0, 0.2 mM ATP, 0.2 mM $CaCl_2$, 0.5 mM mercaptoethanol). The purity was demonstrated by gel electrophoresis (SDS-PAGE). The concentration was determined by amino acid analysis after acid hydrolysis (6 M HCl, 155 °C, 1 h) and precolumn derivatization with *o*-phthaldialdehyde/3-mercaptopropionic acid.[2c] Tβ_4 was a gift from RegeneRx Biopharmaceuticals. Microbial transglutaminase (*Streptomyces mobaraensis*) was a gift from Prof. Pietzsch (MLU, Halle-Wittenberg). Trypsin (proteomic grade, T6667) was obtained from Sigma-Aldrich.

Chemical Cross-Linking. A solution containing 10 μM G-actin and 20 μM Tβ_4 in MES buffer (5 mM MES, pH 6.0) was incubated at room temperature for 15 min. Carbodiimide-mediated cross-linking was initiated by the addition of 1-ethyl-3-(3-dimethylaminopropyl)carbodiimide (EDC) to a final concentration of 0.5 mM. The sample was incubated for 20 h at room temperature, and the reaction was stopped by the addition of SDS reducing buffer followed by SDS-PAGE (Bio-Rad protocol).

Enzymatic Cross-Linking. A solution containing 10 μM G-actin and 20 μM Tβ_4 in phosphate buffer (50 mM Na_2HPO_4/NaH_2PO_4, pH 8.0) was incubated at room temperature for 15 min. Enzymatic cross-linking was performed using microbial transglutaminase (mTGA) in a ratio of 1–2 mU/mg protein. After incubation for 1 h at 37 °C, the reaction was stopped by the addition of SDS reducing buffer followed by SDS-PAGE (Bio-Rad protocol).

Isolation and Tryptic Digestion of Cross-Linked Products. The cross-linked products were isolated by SDS-PAGE (Bio-Rad Mini-Protean Tetra Cell) using 10% gels and stained with Coomassie blue. The gel was kept in water for at least 15 h. Bands of interest were excised and cut into small pieces in a tube. Destaining of the gel pieces was achieved by successive incubation for 30 min at 37 °C with 200 mM NH_4HCO_3, 80 mM NH_4HCO_3/60% acetonitrile (ACN), and 50 mM NH_4HCO_3. Supernatants were removed after each incubation step. Gel pieces were dehydrated by incubation in 100% ACN for 15 min. After the supernatant is removed, the gel pieces were rehydrated in a trypsin solution (20 μg/mL trypsin, 28 mM NH_4HCO_3, 10% ACN) for 1 h on ice and for 20 h at 37 °C. Supernatant was directly analyzed by high-resolution HPLC–ESI–MS.

HPLC–ESI–MS. All common chemicals and reagents were of analytical grade and were purchased from Merck (Darmstadt, Germany) and Sigma-Aldrich (St. Louis, MO, USA). High-resolution HPLC–ESI–MS/MS experiments were carried out using an Ultimate 3000 Micro HPLC apparatus (Dionex, Sunnyvale, CA, USA) equipped with a FLM-3000 flow manager module and coupled to an LTQ Orbitrap XL apparatus (ThermoFisher). A Zorbax 300 SB-C8 (3.5 μm particle diameter; 1 mm i.d. × 15 cm) was used as a chromatographic column.

High-resolution HPLC–ESI–MS/MS experiments were performed on an LTQ Orbitrap XL apparatus using the following eluents for reversed-phase chromatography: 0.1% aqueous formic acid (eluent A) and 0.1% formic acid in acetonitrile–water 80/20 (v/v) (eluent B). The applied gradient was as follows: 0–1 min, 2–12% B; 1–16 min, 12%–65% B (linear); 16–17 min, 65%–100% B (linear). A flow rate of 80 μL/min was used. Mass spectra were collected in data-dependent scan (MS/MS data) mode with a capillary temperature of 250 °C, a sheath gas flow rate of 40 arbitrary unities, a source voltage of 4.0 kV, and a capillary voltage of 48 V. Measurements were performed in the positive ion mode, and mass accuracy (FT) was calibrated before measurements. Selected protein charge states were isolated with a width of m/z 6–10 and activated for 30 ms using 35% normalized collision energy and an activation q of 0.25. All parameters of the tune method were optimized using the standard of Tβ_4.

Molecular Modeling. The X-ray structure of actin was obtained from the protein database (code 3DAW),[11] and the missing three N-terminal residues were added to the protein chain using Sybyl 7.3.[12] Full-length Tβ_4 was set up in two conformations according to experimental findings: completely extended and with two α-helices (D5–L17, K31–A40).[8] After placing Tβ_4 in proximal distance to the interaction sites found by chemical cross-linking, the models were further refined using restrained molecular dynamic simulations with the Amber11 program package.[13] Initial energy minimization (500 steps) reduced potential steric clashes. During the following 200 ps molecular dynamic simulations, Tβ_4 was docked to actin via harmonically restrained interaction distances K3(Tβ_4) ×

dx.doi.org/10.1021/bi400664k | *Biochemistry* 2013, 52, 5553–5562

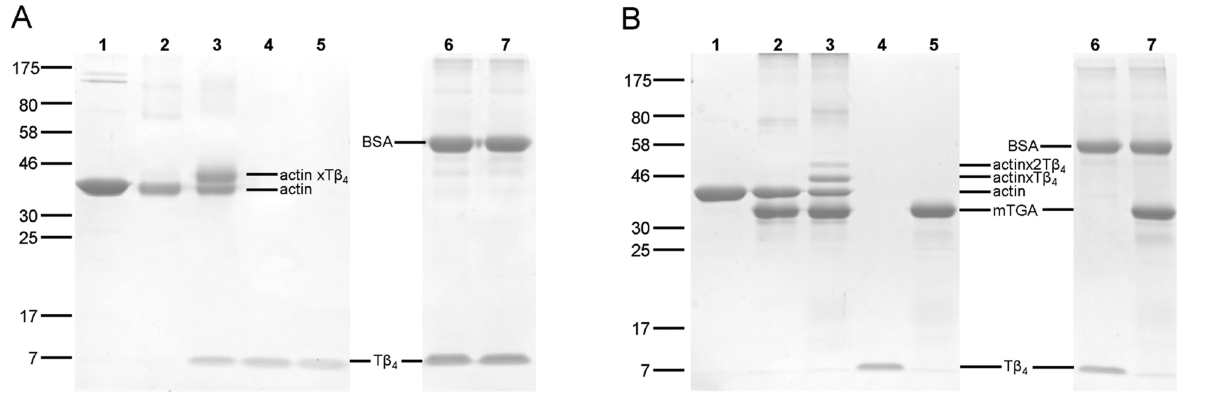

Figure 2. Chemical and enzymatic cross-linking of the actin and Tβ_4. Actin (10 μM) and Tβ_4 (20 μM) were incubated with either EDC (A) or mTGA (B) as described in the methods. Cross-linked products were separated by SDS-PAGE and Coomassie stained. Specificity of the cross-linking reaction was proven by an absence of any cross-linked products using BSA instead of actin. Key: (1) actin; (2) actin + EDC/mTGA; (3) actin + Tβ_4 + EDC/mTGA; (4) Tβ_4; (5) Tβ_4 + EDC/mTGA; (6) BSA + Tβ_4; (7) BSA + Tβ_4 + EDC/mTGA.

E167(actin), K18(Tβ_4) × D1(actin), and S43(Tβ_4) × H40-(actin). To ensure a stable actin conformation, its backbone atoms were also harmonically restrained to their initial coordinates. Calculations used the ff99SB-ILDN parameter set[14] and a generalized Born method for solvation,[15] applying a time step of 2 fs at 300 K and 1 bar. Visualization of structures was performed with VMD.[16]

RESULTS

Characterization of the Reaction Products after Chemical Cross-Linking. EDC is a "zero-length" cross-linker that leads to the formation of isopeptide bonds between carboxy and amine groups in close vicinity. Treatment of G-actin and Tβ_4 with EDC and separation of the peptides using SDS-PAGE shows the formation of a single cross-linked product (Figure 2A). The molecular mass of this product of 47 kDa corresponds to Tβ_4 (5 kDa) bound to actin (42 kDa) in a stoichiometric 1:1 ratio. Under the conditions described, about 50% of the actin becomes cross-linked. Specificity of this cross-linking reaction is proven by the absence of any products using bovine serum albumin (BSA) instead of actin.

Contact Sites in the Actin−Thymosin β_4 Complex by Chemical Cross-Linking. After SDS-PAGE, the bands corresponding to 42 kDa (actin) and 47 kDa (actin−thymosin β_4 complex) were digested using trypsin. The tryptic fragments in the supernatant solutions were analyzed by HPLC−ESI−MS. We were able to identify three tryptic fragments containing a cross-linking site. Using MS/MS data and isotopic modeling, it was possible to localize the contact sites (Figure 3).

The MS/MS data of the first fragment ($[M + H]^+$ = 1643.765 m/z, retention time = 14.8 min) is shown in Figure 3A and corresponds to the product ions of the tryptic fragments Tβ_4(39−43) and actin(40−50). The detection of the product ions $\mathbf{y}_{11}$ and $\mathbf{y}_{12}$ indicated the cross-linking site between the C-terminal carboxyl group of S43(Tβ_4) and the imidazole ring of H40(actin).

The second fragment ($[M + H]^+$ = 2349.159 m/z, retention time = 20.9 min) was assigned to a cross-link between the tryptic fragments Tβ_4 (17−19) and actin(1−18), containing two modifications. The addition of propionamide at C10(actin) caused by nonpolymerized acrylamide during SDS-PAGE led to an increase of the mass of 71.037 Da. Additionally, deamidation at N12(actin) caused a mass increase of 0.984 Da. The cross-linking site and the modifications were verified by the MS/MS spectrum (Figure 3B). Detection of the product ion $\mathbf{b}_6$ suggested the cross-link site to be between the ε-amino group at K18 or K19 of Tβ_4 and a free carboxyl group at one of the first three amino acids of actin (DDE).

The third fragment ($[M + H]^+$ = 4482.210 m/z, retention time = 27.7 min) resulted from a cross-link between the N-terminal tryptic fragments Tβ_4 (1−11) and actin(148−177). The product ions of the MS/MS spectrum (Figure 3C) corresponded with parts of the **b** and **y** series of these tryptic fragments. Due to the detection of the product ion $\mathbf{y}^*_8$, a cross-link containing E8, E10, or K11 of Tβ_4 could be excluded. The product ion $\mathbf{y}^*_9$ included the additional mass for the tryptic fragment actin(148−177). Therefore, only K3(Tβ_4) was eligible as the amine donor. The detection of the product ions $\mathbf{b}_{16}$ and $\mathbf{y}_{10}$ identified E167(actin) as the acyl donor.

Concomitant to the detection of these three fragments containing the cross-linking site, the corresponding non-cross-linked tryptic fragments were also identified. The relative intensity of the cross-linked fragments was only 1.5−21%, whereas for non-cross-linked fragments it was 14−75% (Table 1).

Characterization of the Reaction Products after Enzymatic Cross-Linking. In contrast to chemical cross-linking with EDC, the enzymatic cross-linking reaction between actin and Tβ_4 using mTGA led to the formation of different products. SDS-PAGE was used to separate the two cross-linked products (see Figure 2B); on the basis of the band at 42 kDa representing actin, the bands of the cross-linked products are visible in distances of 5 and 10 kDa. This indicates the cross-linking of one and two molecules of Tβ_4 to actin.

Contact Sites in the Actin−Thymosin β_4 Adduct by Enzymatic Cross-Linking. Analogous to the identification of contact sites after EDC treatment, the bands of interest were excised from the gel, digested with trypsin, and analyzed using HPLC−ESI−MS. Three tryptic fragments containing cross-linking sites were identified by a comparison of the data of non-cross-linked actin and that of the 1:1 adduct (Figure 4).

The first fragment ($[M + H]^+$ = 1827.801 m/z, retention time = 12.7 min) was assigned to a cross-link between the tryptic fragments actin(51−62) and Tβ_4 (39−43). The cross-link was confirmed by the MS/MS spectrum (Figure 4A), which indicated that the product ions of the parent ion (1827.798 Da) correlated with parts of the **b** and **y** series of both actin(51−62) and Tβ_4(39−43) fragments. The cross-

dx.doi.org/10.1021/bi400664k | Biochemistry 2013, 52, 5553−5562

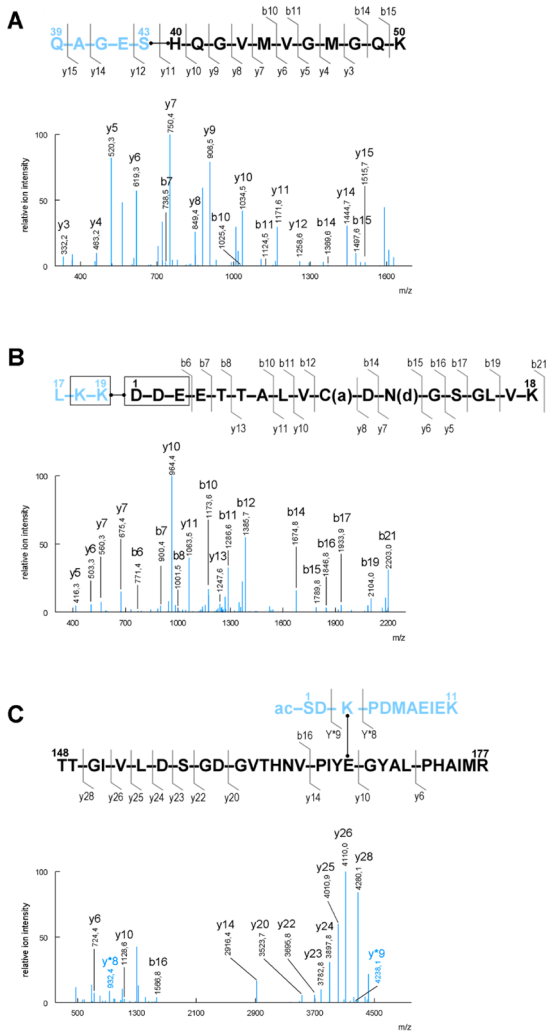

Figure 3. Contact sites in the actin−Tβ_4 complex after chemical cross-linking using EDC. MS/MS spectra and the sequence of the cross-linked fragments corresponding to the parent ions are shown: (A) $[M + H]^+$ 1643.765 m/z, (B) $[M + H]^+$ 2349.159 m/z, and (C) $[M + H]^+$ 4482.210 m/z. Tryptic fragments of actin are marked in black; fragments of Tβ_4 are marked in blue. (A) The MS/MS spectrum confirms the cross-linking site between the C-terminal carboxy group at S43 of Tβ_4 and the imidazole ring at H40 of actin. (B) The MS/MS spectrum corresponds to the cross-linking product of the tryptic peptides 1−18 of actin and 17−19 of Tβ_4. Two modifications were identified in the actin peptide: propionamide modification at C10 (+71.039 Da) and deamidation at N12 (+0.98 Da). The carboxy group of one of the amino acids 1−3 of actin is cross-linked to K18 or K19 of Tβ_4. (C) The MS/MS spectrum confirms the cross-linking site between the carboxy group at E167 of actin and the ε-amine group at K3 of Tβ_4.

linking reaction of the mTGA leads to the formation of isopeptide bonds only between ε-amino groups and γ-carbamoyl groups of lysine and glutamine side chains. Therefore, the cross-linking site could only be located between Q39(Tβ_4) and K61(actin). This was confirmed by the $\mathbf{b}^*_2$ and $\mathbf{y}_3$ ions. The mass of the product ion $\mathbf{b}^*_2$ of the Tβ_4 fragment was increased by the fragment actin(51−62). The product ion $\mathbf{y}_3$ of the actin fragment additionally consisted of the peptide Tβ_4(39−42).

The second fragment ($[M + H]^+$ = 2016.987 m/z, retention time = 13.2 min) corresponded to a cross-link site between the

Table 1. Identified Tryptic Fragments of the EDC-Cross-Linked Actin−Tβ_4 Complex[a]

retention time, min	tryptic fragments	intensity	m/z theoretical	m/z experimental	$\delta m/m$,[b] ppm
5.2	A207−210	0.41	516.314	516.315	1.94
6.2	T32−38	0.65	876.431	876.433	2.40
9.6	T26−31	1.73	655.377	655.379	2.44
10.1	A192−196	4.78	631.377	631.378	0.95
11.0	A51−61	31.34	1198.522	1198.526	3.17
11.0	A285−290	3.21	734.350	734.333	−23.42
12.3	T20−31	1.94	1371.711	1371.714	1.90
12.3	A329−336	0.38	923.567	923.569	1.84
13.4	A19−28	32.43	976.448	976.451	2.77
14.2	A329−335	21.78	795.472	795.474	2.14
14.5	A178−183	27.23	644.373	644.373	0.62
14.6	A40−50	17.83	1171.571	1171.573	1.62
14.8	**A40−50 × T39−43**[c]	**4.77**	**1643.772**	**1643.765**	**−4.26**
15.6	T26−38	26.63	1512.790	1512.794	2.38
16.3	A360−372	36.84	1500.708	1500.713	3.53
16.8	T1−11[d]	33.78	1304.604	1304.606	1.61
19.2	A197−206	46.90	1130.548	1130.551	2.92
19.7	A316−326	41.10	1161.618	1161.622	3.10
20.4	A85−95	28.07	1515.749	1515.754	3.17
20.9	A63−68	8.29	644.434	644.435	1.40
20.9	**A1−18 × T17−19**[c,c]	**2.98**	**2349.152**	**2349.159**	**2.94**
21.5	T1−14[d]	70.37	1694.794	1694.801	4.01
22.1	A29−39	34.98	1198.706	1198.707	1.25
22.2	A1−18[cd],	14.38	1978.891	1978.893	1.06
23.0	A96−113	210.36	1956.044	1956.051	3.73
24.9	A184−191	35.91	998.486	998.489	2.70
25.6	A239−254	168.39	1790.892	1790.895	1.73
26.1	A69−84[f]	141.37	1974.919	1974.935	8.24
27.7	**A148−177 × T1−11**[c]	**1.18**	**4482.203**	**4482.210**	**1.58**
28.4	A148−177	75.55	3196.610	3196.625	4.82
31.4	A257−284[e]	0.97	3202.489	3202.497	2.40
46.9	A119−147	4.31	3251.630	3251.632	0.55

[a]Cross-linking reaction by EDC was performed in a molar ratio of 1:2 for 20 h at rt. The reaction mixture was separated by SDS-PAGE, and bands of interest were digested with trypsin and analyzed by HPLC−ESI−MS. [b]$\delta m/m$ = (m/z experimental − m/z theoretical)/(m/z theoretical). [c]Cross-linking sites. [d]Acetylation at protein N-terminus. [e]Propionamide modification at cysteine. [f]Methylhistidine.

tryptic fragments actin(40−50) and Tβ4(19−25). The cross-linking was verified by the correlation of the product ions of the MS/MS spectrum (Figure 4B) with parts of the **b** and **y** series of both fragments. The fragments of Tβ_4, as well as of actin, included putative lysine and glutamine residues that might be involved in the enzymatic reaction. However, detection of the $\mathbf{y}^*_6$ and $\mathbf{b}_2$ ions clearly indicated the cross-link to be between Q41(actin) and K19(Tβ $_4$). The $\mathbf{y}^*_6$ ion only included the amino acid residues 20−25 of Tβ_4. Thus, the residues Q23 and K25 could be excluded. The ion $\mathbf{b}_2$ represented the peptide actin(40−41) and was increased by the mass of the peptide Tβ_4(19−25). Therefore, only Q41(actin) was cross-linked, not the also-possible residue Q49(actin).

The third contact site was identified by the fragment ($[M + H]^+$ = 2230.133 m/z, retention time = 14.9 min). This is a cross-link of higher order. The tryptic fragment Tβ_4(15−19)

dx.doi.org/10.1021/bi400664k | *Biochemistry* 2013, 52, 5553−5562

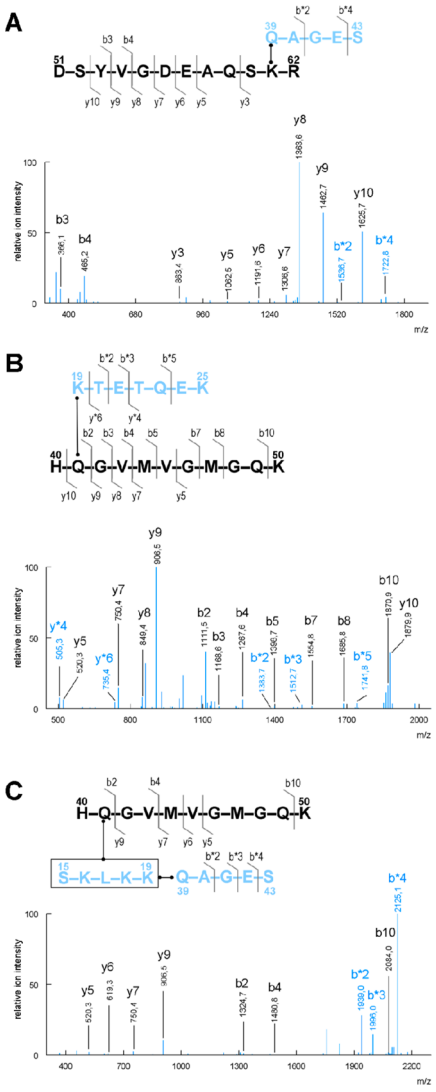

Figure 4. Contact sites in the actin−Tβ_4 adduct after enzymatic cross-linking using mTGA. MS/MS spectra and the sequence of the cross-linked fragments are shown. Tryptic fragments of actin are marked in black; fragments of Tβ_4 are marked in blue. (A) The MS/MS spectrum, sequence, and fragmentation pattern of the peptide 51−62 of actin cross-linked to 39−43 of Tβ_4 corresponding to the parent ion, $[M + H]^+$ 1827.801 m/z. The cross-linking site was identified between the Q39 of Tβ_4 and the ε-amine group at K61 of actin. (B) The MS/MS spectrum of the parent ion $[M + H]^+$ 2016.987 m/z corresponding to peptides 40−50 of actin and 19−25 of Tβ_4. The **b** and **y** ion series indicate a cross-linking site between Q41 of actin and K19 of Tβ_4. (C) The MS/MS spectrum of the parent ion, $[M + H]^+$ 2230.133 m/z, corresponding to a cross-link between fragments 40−50 of actin, 39−43 of Tβ_4, and 15−19 of Tβ_4. Q41 of actin and Q39 are simultaneously cross-linked to K16, K18, or K19 of Tβ_4.

was simultaneously cross-linked to two other tryptic fragments: actin(40−50) and Tβ_4(39−43). The product ions of the MS/MS spectrum (Figure 4C) corresponded to parts of the **b** and **y** series of two of these fragments: actin(40−50) and Tβ_4(39−43). Neither **b** nor **y** series ions were detected for the fragment Tβ_4(15−19). However, the **y** series ions of the peptide actin(40−50) and the **b*** series ions of Tβ_4(39−43) were exactly increased by the mass of the doubled cross-linked peptide Tβ_4(15−19). Detection of the $\mathbf{y_9}$ ion indicated the cross-link at Q41(actin) and excluded Q49 and K50. Because Tβ_4(39−43) does not contain lysine residues, Q41(actin) must have been cross-linked to one of the three lysine residues in Tβ_4(15−19). Additionally, the only residue eligible for cross-linking in the peptide Tβ_4(39−43) is Q39. The detection of the $\mathbf{b^*_2}$ and $\mathbf{b^*_4}$ ions verified the cross-link between Q39 and one of the three lysine residues 16, 18, or 19 of Tβ_4.

Analogous to the chemical cross-linking, the enzymatic cross-linking also led to the concomitant detection of the cross-linked fragments and the corresponding non-cross-linked fragments. The intensity of the cross-linked fragments was between 0.8 and 4.3%, whereas the corresponding fragments had intensities between 2.3 and 20.2% (Table 2).

Table 2. Identified Tryptic Fragments of the mTGA-Cross-Linked Actin−Tβ_4 Complex[a]

retention time, min	trypsin fragment	intensity	m/z theoretical	m/z experimental	$\delta m/m$,[b] ppm
5.3	A207−210	1.03	516.314	516.315	1.94
6.2	T32−38	0.61	876.431	876.432	1.26
9.7	T26−31	1.14	655.377	655.378	0.92
10.2	A192−196	6.51	631.377	631.378	0.95
11.0	A51−61	20.23	1198.522	1198.524	1.50
11.0	A285−290	2.46	734.350	734.332	−24.78
12.2	T20−31	0.40	1371.711	1371.714	1.90
12.5	A329−336	0.42	923.567	923.569	1.84
12.7	**A51−62 × T39−43**[c]	**0.76**	**1827.798**	**1827.801**	**1.70**
13.2	**A40−50 × T19−25**[c]	**4.32**	**2016.983**	**2016.987**	**1.98**
13.4	A19−28	44.39	976.448	976.451	2.77
14.2	A329−335	31.51	795.472	795.474	2.14
14.5	A178−183	47.97	644.373	644.373	0.62
14.9	**A40−50 × T39−43**[c] **× T15−19**	**3.00**	**2230.130**	**2230.133**	**1.57**
14.9	A40−50	2.31	1171.571	1171.572	0.77
15.5	T26−38	4.84	1512.790	1512.792	1.06
16.1	A360−372	46.68	1500.708	1500.712	2.87
16.8	T1−11[d]	20.29	1304.604	1304.606	1.61
19.2	A197−206	54.91	1130.548	1130.549	1.15
19.6	A316−326	48.68	1161.618	1161.621	2.24
20.4	A85−95	29.42	1515.749	1515.753	2.51
21.0	A63−68	11.83	644.434	644.435	1.40
21.5	T1−14[d]	48.45	1694.794	1694.800	3.42
22.1	A29−39	32.28	1198.706	1198.706	0.42
22.9	A1−18[d,e,c]	28.28	1979.871	1979.882	5.61
23.0	A96−113	174.65	1956.044	1956.050	3.22
24.8	A184−191	52.75	998.486	998.489	2.70
25.5	A239−254	182.56	1790.892	1790.893	0.61
26.1	A69−84[f]	137.20	1974.919	1974.934	7.74
26.1	A292−312	72.29	2228.065	2228.068	1.26
28.4	A148−177	79.53	3196.610	3196.623	4.19
31.1	A216−238[e]	0.50	2550.174	2550.179	2.08
31.5	A257−284[e]	2.17	3202.489	3202.495	1.78
45.5	A337−359	0.36	2602.337	2602.341	1.38
46.8	A119−147	4.24	3251.630	3251.632	0.55

[a]Cross-linking reaction by mTGA was performed in a molar ratio of 1:2 for 1 h at 37 °C. The reaction mixture was separated by SDS-PAGE, and bands of interest were digested with trypsin and analyzed by HPLC−ESI−MS. [b]$\delta m/m$. (m/z experimental − m/z theoretical)/(m/z theoretical). [c]Cross-linking sites. [d]Acetylation at protein N-terminus. [e]Propionamide modification at cysteine. [f]Methylhistidine.

dx.doi.org/10.1021/bi400664k | *Biochemistry* 2013, 52, 5553−5562

Generation of a Theoretical Model for the Actin−Tβ_4 Complex from Cross-Linking Data. Molecular modeling was applied to generate a visual model from the information obtained via the cross-linking experiments. Because chemical cross-linking yielded three distinct contact sites located in three actin subdomains, Tβ_4 spans a large distance on the surface of actin. In order to verify that the experimental findings are in accordance with steric conditions in the complex, this input was used as an external restraint upon model building.

We tested a completely extended conformation of Tβ_4, contacting the subdomains 1 to 3 of actin. The model obtained verifies that a concomitant interaction between Tβ_4 and actin at all three cross-linking sites is sterically possible (Figure 5A).

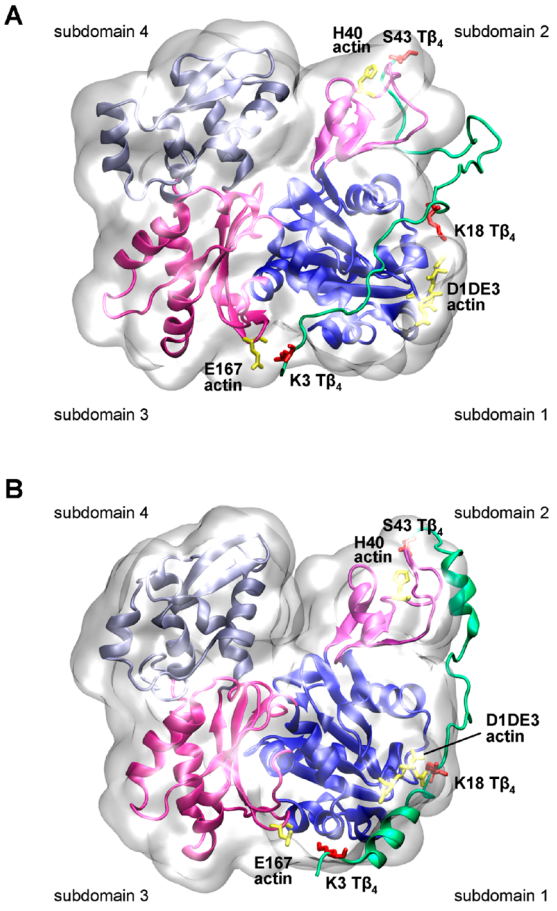

Figure 5. 3D presentation of the actin−Tβ_4 complex. Molecular modeling of the complex between actin and Tβ4 (green), when the identified contact sites by chemical cross-linking are considered, is presented. Amino acid residues involved in the chemical cross-linking reaction are labeled and highlighted. (A) Extended conformation of Tβ_4 contacting the subdomains 1 to 3 of actin. The model obtained verifies that a concomitant interaction between Tβ_4 and actin at all three identified contact sites after chemical cross-linking is sterically possible. (B) The second model for the actin−Tβ_4 complex including NMR studies of Domanski et al. with a Tβ_4 conformation that contained two helical parts between residues 6−13 and 31−40 upon binding to actin is presented.[8] The contact sites identified via chemical cross-linking are also compatible with Tβ_4 exhibiting helical regions.

The distance of the N-terminal region between amino acids 4−17 and of the C-terminal region between amino acids 19−42 of Tβ_4 is much larger than required to fit the cross-linking sites at the N-terminus, H40 and E167 of actin. Hence, it is possible that secondary structures within Tβ_4 are formed in these regions.

NMR studies performed by Domanski et al. showed that Tβ_4 forms two helices between residues 5−17 and 31−40 upon binding to actin.[8] We, therefore, created a second model for the actin−Tβ_4 complex starting with a Tβ_4 conformation that contained two helical parts. From Figure 5B, it can be seen that the contact sites identified via cross-linking are also compatible with Tβ_4 exhibiting helical regions.

DISCUSSION

Identification of Contact Sites in the Actin−Tβ_4 Complex after Chemical Cross-Linking. Using mass spectrometric analyses of the tryptic digests of the chemically cross-linked actin−Tβ_4 complex, we were able to identify three contact sites: one of the first three amino acid residues (D1, D2, E3) of actin is cross-linked to K18 or K19 of Tβ_4; H40(actin) is cross-linked to the C-terminal carboxy group of S43(Tβ_4); the third contact site was identified between E167(actin) and K3(Tβ_4).

The cross-linking sites were found in tryptic fragments including partial sequences of both actin and Tβ_4. When we assume that all three identified contact sites are cross-linked concomitantly, the corresponding non-cross-linked partial sequences of actin and Tβ_4 should not be observed in the same sample. The fact that we were able to detect both, cross-linked and the corresponding non-cross-linked partial sequences, suggests that the identified contact sites are not exclusively cross-linked at the same time. Therefore, the actin−Tβ_4 complex must consist of different products after chemical cross-linking. There is, however, still an equal composition of one molecule of Tβ_4 cross-linked to one molecule of actin. The variability of cross-linking also explains the weak intensity of the three cross-linked fragments. Additional cross-linking sites might also be formed but evade identification due to an even lower intensity.

The actin molecule is divided into four subdomains. The three contact sites identified reside on subdomains 1 to 3. One of the contact sites (E167(actin) × K3(Tβ_4)) is in accordance with the data of Safer et al.[9a] A second contact site found in the same working group, D1-E4(actin) × K18(Tβ_4), was identified here in a modified state, D1-E3(actin) × K18/K19(Tβ_4). Furthermore, Safer et al. identified a third contact site in the complex between Q41(actin) and K38(Tβ_4) using tissue transglutaminase. From this, they postulated an extended conformation of Tβ_4 to contact both the barbed and the pointed end of actin. We were able to confirm this suggestion by the identification of a third contact site between the C-terminus of Tβ_4 and H40 of actin on subdomain 2 after chemical cross-linking.

De La Cruz et al. were also able to chemically cross-link the C-terminus of Tβ_4 to H40(actin). They used an engineered Tβ_4 construct S43C(Tβ_4) and a chemical cross-linker *N*,*N*-9-*o*-phenylenedimaleimide (oPDM). oPDM is a homobifunctional cross-linker that forms bridges between sulfhydryl groups with a spacer length of 9.4 Å,[17] which is in contrast to our investigations because we showed a "zero-length" distance between the C-terminus of Tβ_4 and H40(actin) using the unmodified Tβ_4.

Reichert et al. studied the binding between Tβ_4 and actin using a bifunctional thiol cross-linker with different spacer lengths.[9b] Formation of a disulfide bridge between actin and cysteine side chains of different Tβ_4 mutants succeeded

dx.doi.org/10.1021/bi400664k | *Biochemistry* 2013, 52, 5553−5562

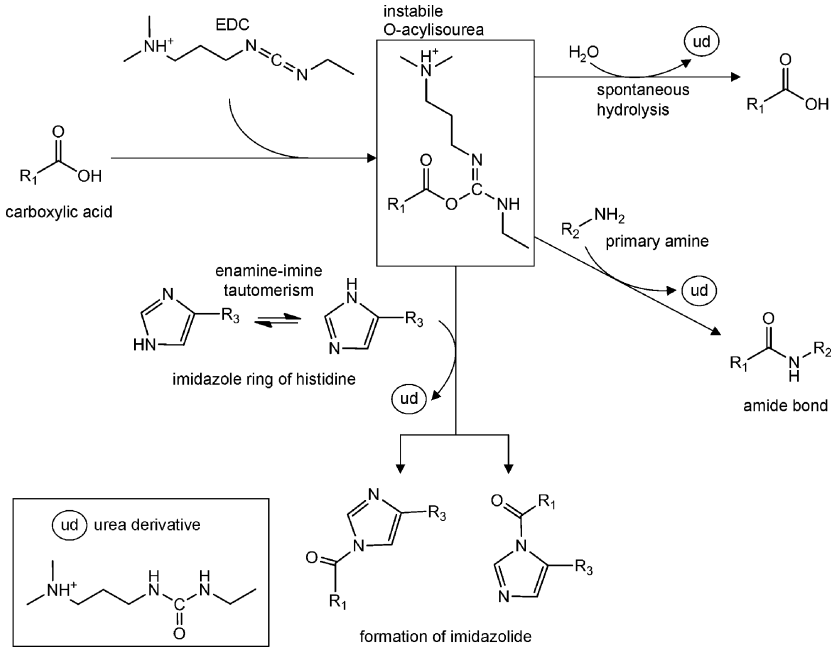

Figure 6. Reaction mechanism of chemical cross-linking reaction by EDC. EDC reacts with carboxylic acid to unstable *O*-acyl-isourea. By spontaneous hydrolysis, the carboxylic acid is regenerated. In the presence of primary amines, amide bonds are formed. In this study, we first provide evidence that EDC leads to the formation of imidazoles by cross-linking carboxylic acids with the imidazole ring of histidine.

between residue 6 of Tβ_4 and C374(actin) with a spacer length of 18 Å. In our model, this distance is comparable to a spacer length of about 19 Å. Reichert et al. also identified additional disulfide bridges between amino acids 17 and 28 of Tβ_4 with the actin-bound ATP analogon with spacer lengths of 9 and 18 Å, respectively. In our model, these distances are between 27 and 35 Å. An explanation of these discrepancies could be the high flexibility of Tβ_4. Using the HPLC–ESI–MS data, we were able to see that the three identified cross-linking sites are not always formed concomitantly. It is possible that Tβ_4 flexibly binds to different regions of actin and that, for instance, the binding to central parts of the actin molecule, in the vicinity of the central ATP, was not detectable with our methods.

Wiskott–Aldrich Syndrome protein (WASp) homology domain 2 (WH2) is an actin monomer binding motif. Tβ_4 shares structural similarity with the WH2 domain; however, WH2 lacks the C-terminal region of Tβ_4 and binds to actin more strongly than Tβ_4. Additionally, the WH2-containing proteins are folded.[18] The WH2 domain consists of a N-terminal α-helix followed by the preserved LKKT linker related to Tβ_4. The N-terminal helix of the WH2 domain binds to the actin cleft between subdomains 1 and 3.[19] This is comparable to our results showing a cross-link between K3 of the N-terminal region of Tβ_4 and E167 of subdomain 3 of actin close to subdomain 1. The LKKT linker of the WH2 domain binds close to the central nucleotide-binding cleft.[19a] This is in accordance with the results of Reichert et al., who were able to cross-link the central part of Tβ_4 to an ATP analogon.[9b] In contrast, our results showed that the central part of Tβ_4 is bound to the N-terminus of actin on subdomain 1. Hertzog et al. created a 3D model of the actin–Tβ_4 complex by assignment of the X-ray data of the crystallized actin–ciboulot D1 complex.[19b] This complex shows, in accordance to other WH2 domains, the contact site of the central part of Tβ_4 close to the nucleotide binding cleft of actin. Ciboulot is a three-WH2 domain repeat protein, although only the first repeat D1 binds actin. D1 shares 14 identical amino acids with Tβ_4 consisting of 43 amino acids. The differences in the sequences could be the reason for the deviations of the contact site for the central part of Tβ_4.

The Imidazole Ring of Histidine Serves as Acyl Acceptor for EDC-Mediated Cross-Linking. The "zero-length" cross-linker EDC leads to the formation of isopeptide bonds between carboxyl groups (acyl donor) and secondary amine groups (acyl acceptor). The identified cross-linking site, S43(Tβ_4) × H40(actin), possesses a special character because the amine donor is a primary amino group of the imidazole ring of histidine. We, thus, provide the first evidence for the imidazole ring of histidine residues becoming the amine donor for chemical cross-linking using EDC (Figure 6). The molar ratio of the imidazole tautomers is highly dependent on surrounding structures in the protein and the pH value of the environment.[20] Therefore, it is not possible to predict which nitrogen of the imidazole ring reacts preferentially.

Model of the Actin–Tβ_4 Complex. The identified cross-linking sites allowed us to devise a structural model of the actin–Tβ_4 complex using molecular modeling. Although the three contact sites were not necessarily occupied at the same time in the complex according to the MS data, we decided to use this special case for two reasons: first, three distance restraints reduced the conformational space of Tβ_4 significantly during complex modeling; second, we wanted to test whether the peptide length would allow for simultaneous contact of all sites identified. As Tβ_4 is known to form two α-helices upon binding to actin,[8] the models of the complex with Tβ_4 in two different conformations might well represent structures at different stages of complexation. However, as the three identified contact sites were not always formed concomitantly, it is possible that Tβ_4 changed its binding position after secondary structure formation. At least one such alternative binding position of Tβ_4 can be deduced from its similarity to WH2 domains in terms of amino acid sequence and

dx.doi.org/10.1021/bi400664k | *Biochemistry* 2013, 52, 5553–5562

modulation of ADP/ATP binding.[19] This suggested a similar binding pattern for both species, where the central part of Tβ_4 formed contacts close to the nucleotide binding cleft, and further demonstrated the structural complexity of the actin−Tβ_4 complex.

Implications of the Identified Contact Sites for Further Interactions. The sequestering of G-actin by Tβ_4 inhibits its polymerization from G-actin monomers to filamentous F-actin. This mechanism results from masking important regions of actin that are necessary for intermolecular interactions in the process of polymerization. These interaction regions are investigated and defined in different studies. The first model of F-actin was published by Holmes et al.[21] Oda et al. extended this model almost 20 years later.[22] The contact sites between the actin molecules in F-actin overlap on both models. In line with our identified cross-linking sites are two intersection points: K3(Tβ_4) is cross-linked to E167(actin), which is part of the section (166−169) involved in important interactions within F-actin, according to Holmes et al. The C-terminus of Tβ_4 binds to H40 of actin, which is part of the contact site identified in F-actin in both models of Holmes et al. (residues 39−45 of actin) and Oda et al. (residues 38−49 of actin). Additionally, Oda et al. identified the actin region 39−42 as an important interaction site between the two polymerization chains within F-actin.

The cross-linking site at H40(actin) identified here is also part of the binding region of DNase I.[23] DNase I leads to the depolymerisation of F-actin due to the formation of stable DNase I−actin complexes; thereby, the enzymatic activity of DNase I gets lost.[23b] The competition of Tβ_4 for the same binding site could displace DNase I from the complex with actin. This is pharmacologically important considering the fact that DNase I is used to treat cystic fibrosis. The loss of enzymatic activity of DNase I after binding actin in sputum could be reversed by Tβ_4. Simultaneously, Tβ_4 can inhibit polymerization of actin and, therefore, lower the viscosity of sputum along with DNase I.[24]

Reichert et al. contradict this assumption.[25] In their studies, the activity of DNase I in the presence of chemically cross-linked actin−Tβ_4 complex was equally well inhibited compared to that of actin. In their experiments, the mutant M6C(Tβ_4) was cross-linked to actin using the bifunctional thiol cross-linker. It is possible that the mutation influences the conformation of the complexed Tβ_4 so that Tβ_4 does not bind to the contact site of DNase I.

Studies of Ballweber et al. showed that it is impossible to chemically cross-link actin simultaneously with Tβ_4 and profilin. In contrast, it is possible to form a ternary complex between actin, DNase I, and profilin.[26] These results are explained by our identified cross-linking sites between Tβ_4 and actin. Profilin binds actin at subdomains 1 and 3.[27] This contact site overlaps that of Tβ_4, which binds to subdomains 1−3 of actin. Therefore, a ternary complex is not possible. DNase I binds actin at subdomain 2, outside the binding site for profilin. Thus, the formation of the ternary complex between actin, DNase I, and profilin is possible.

Identification of Contact Sites in the Actin−Tβ_4 Adduct after Enzymatical Cross-Linking. Tβ_4 and actin were enzymatically cross-linked using mTGA. This enzyme is a member of the enzyme class of protein-glutamine γ-glutamyltransferases, like the blood coagulation factor XIIIa. It has been shown that actin is incorporated in the fibrin clot by factor XIIIa during the blood coagulation cascade in vivo.[28] It has also been shown that Tβ_4 is a substrate of factor XIIIa.[29] Therfore, it is possible that the enzymatic cross-linking between Tβ_4 and actin also proceeds in vivo.

We are able to identify three different cross-linking sites in the enzymatic cross-linking product of Tβ_4 and actin: K61(actin) × Q39(Tβ_4), Q41(actin) × K19(Tβ_4), and Q41(actin) + Q39(Tβ_4) are simultaneously cross-linked to K16, K18, or K19 of Tβ_4. In addition to fragments containing the cross-linking site, the corresponding non-cross-linked fragments are also identified. This indicates that the cross-linking sites are not necessarily formed concomitantly. In contrast to chemical cross-linking, enzymatic cross-linking leads to the formation of various cross-linked products. Although the product consisting of one molecule of Tβ_4 linked to one molecule of actin has the highest intensity, the intensity of additional products decreases with the number of additionally incorporated Tβ_4 molecules to the adduct. It was not possible to identify additional cross-linking sites for further incorporating Tβ_4 molecules, so it remains unclear if additional Tβ_4 molecules are cross-linked to actin or to the already cross-linked Tβ_4.

Safer et al. localized a different enzymatic cross-linking site in the actin−Tβ_4 adduct using tissue transglutaminase: Q41-(actin) × K38(Tβ_4).[9a] An explanation of this discrepancy could be the different specificity of microbial and the Ca^{2+}-dependent tissue transglutaminase. Huff et al. presented Q23 and Q36 of Tβ_4 as preferred glutaminyl substrates of tissue transglutaminase, whereas Q39(Tβ_4) reacted with a low efficiency.[30] Our results using mTGA, however, showed a preferred reaction at Q39(Tβ_4). Additionally, Tβ_4 also reacted as amine substrate at K19 and K16 or K18.

The cross-linking site between Q41 of actin and K19 of Tβ_4 is reminiscent of the work of Eligula et al., who also investigated cross-linking between actin and myosin using mTGA.[31] Analogous to our results and the results of Safer et al., Q41(actin) was always involved in the cross-linking reaction. Myosin includes a lysine-rich region in the S1 part of the heavy chain between amino acid residues 636 and 642. This region is cross-linked using mTGA to Q41(actin) and bears a certain similarity to the lysine-rich region in the Tβ_4 molecule; the central part of Tβ_4 between the amino acid residues 14 and 19 includes four lysines.

Furthermore, the interaction between actin and cofilin was investigated using mTGA. Again, Q41 of subdomain 2 of actin is involved in the cross-linking reaction.[32] Like Tβ_4, cofilin is an actin-binding protein and fragments F-actin into shorter filaments. The binding of cofilin to subdomain 2 of actin was supported via other experimental methods applied by Kamal et al.; they demonstrated the binding of cofilin to subdomains 1 and 2 of actin.[33] These results also confirm the use of cross-linking reactions with mTGA for the successful identification of protein−protein interactions.

SUMMARY

EDC-mediated chemical and enzymatic cross-linking combined with tryptic digestion and HPLC−ESI−MS analyses have been shown to be an effective strategy in identifying the binding sites in the actin−Tβ_4 complex. Both types of cross-linking yielded the C-terminus of Tβ_4 covalently bound to subdomain 2 of actin. Chemical cross-linking using EDC additionally identified the lysine-rich central part of Tβ_4 binding to the N-terminus (subdomain 1) of actin, whereas enzymatic cross-linking showed Tβ_4 binding to subdomain 2 of actin. Interestingly,

dx.doi.org/10.1021/bi400664k | Biochemistry 2013, 52, 5553−5562

enzymatic cross-linking could not identify a contact site at the N-terminal region of $T\beta_4$, whereas treatment with EDC leads to cross-linking with subdomain 3 of actin.

Both cross-linking procedures are commonly used for identification of protein−protein interactions. An explanation for the differing results could be the highly flexible character of $T\beta_4$. In an aqueous solution, the peptide is unstructured and binding to actin induces formation of structured helices in N- and C-terminal regions.[8,34] Using molecular modeling, we demonstrated that the contact sites identified are compatible with the structural features of the actin−$T\beta_4$ complex. Here, we identified actin and $T\beta_4$ as both lysyl and glutaminyl substrates of mTGA. Interestingly, we found that the imidazole ring of histidine side chains is the acyl acceptor for the chemical cross-linking reaction using EDC.

Our results demonstrate the complex interaction between actin and $T\beta_4$, with distinct contact sites localized on different actin subunits. Thus, they may help to understand the subtle molecular mechanism by which $T\beta_4$ acts as a sequestering agent for actin in its physiological environment.

AUTHOR INFORMATION

Corresponding Author

*E-mail: thymosin@biochem.uni-erlangen.de. Phone: 0049 9131 852 4187.

Notes

The authors declare no competing financial interest.

REFERENCES

(1) Hannappel, E., and van Kampen, M. (1987) Determination of thymosin b_4 in human blood cells and serum. *J. Chromatogr. 397*, 279−285.

(2) (a) Hannappel, E., Davoust, S., and Horecker, B. L. (1982) Thymosins beta 8 and beta 9: two new peptides isolated from calf thymus homologous to thymosin beta 4. *Proc. Natl. Acad. Sci. U. S. A. 79* (6), 1708−1711. (b) Hannappel, E., Wartenberg, F., and Bustelo, X. R. (1989) Isolation and characterization of thymosin beta 9 Met from pork spleen. *Arch. Biochem. Biophys. 273* (2), 396−402. (c) Hannappel, E., Kalbacher, H., and Voelter, W. (1988) Thymosin beta 4Xen: a new thymosin beta 4-like peptide in oocytes of Xenopus laevis. *Arch. Biochem. Biophys. 260* (2), 546−551. (d) Erickson-Viitanen, S., and Horecker, B. L. (1984) Thymosin beta 11: a peptide from trout liver homologous to thymosin beta 4. *Arch. Biochem. Biophys. 233* (2), 815−820. (e) Low, T. L., Liu, D. T., and Jou, J. H. (1992) Primary structure of thymosin beta 12, a new member of the beta-thymosin family isolated from perch liver. *Arch. Biochem. Biophys. 293* (1), 32−39. (f) Stoeva, S., Horger, S., and Voelter, W. (1997) A novel beta-thymosin from the sea urchin: extending the phylogenetic distribution of beta-thymosins from mammals to echinoderms. *J. Pept. Sci. 3* (4), 282−290.

(3) (a) Jean, C., Rieger, K., Blanchoin, L., Carlier, M. F., Lenfant, M., and Pantaloni, D. (1994) Interaction of G-actin with thymosin beta 4 and its variants thymosin beta 9 and thymosin beta met9. *J. Muscle Res. Cell Motil. 15* (3), 278−286. (b) Carlier, M. F., Jean, C., Rieger, K. J., Lenfant, M., and Pantaloni, D. (1993) Modulation of the interaction between G-actin and thymosin beta 4 by the ATP/ADP ratio: possible implication in the regulation of actin dynamics. *Proc. Natl. Acad. Sci. U. S. A. 90* (11), 5034−5038. (c) Hannappel, E., and Wartenberg, F. (1993) Actin-sequestering ability of thymosin beta 4, thymosin beta 4 fragments, and thymosin beta 4-like peptides as assessed by the DNase I inhibition assay. *Biol. Chem. Hoppe-Seyler 374* (2), 117−122.

(4) Dominguez, R., and Holmes, K. C. (2011) Actin structure and function. *Annu. Rev. Biophys. 40*, 169−186.

(5) Welch, M. D., Mallavarapu, A., Rosenblatt, J., and Mitchison, T. J. (1997) Actin dynamics in vivo. *Curr. Opin. Cell Biol. 9* (1), 54−61.

(6) Safer, D., Elzinga, M., and Nachmias, V. T. (1991) Thymosin beta 4 and Fx, an actin-sequestering peptide, are indistinguishable. *J. Biol. Chem. 266* (7), 4029−4032.

(7) Irobi, E., Aguda, A. H., Larsson, M., Guerin, C., Yin, H. L., Burtnick, L. D., Blanchoin, L., and Robinson, R. C. (2004) Structural basis of actin sequestration by thymosin-beta4: implications for WH2 proteins. *EMBO J. 23* (18), 3599−3608.

(8) Domanski, M., Hertzog, M., Coutant, J., Gutsche-Perelroizen, I., Bontems, F., Carlier, M. F., Guittet, E., and van Heijenoort, C. (2004) Coupling of folding and binding of thymosin beta4 upon interaction with monomeric actin monitored by nuclear magnetic resonance. *J. Biol. Chem. 279* (22), 23637−23645.

(9) (a) Safer, D., Sosnick, T. R., and Elzinga, M. (1997) Thymosin beta 4 binds actin in an extended conformation and contacts both the barbed and pointed ends. *Biochemistry (Moscow) 36* (19), 5806−5816. (b) Reichert, A., Heintz, D., Echner, H., Voelter, W., and Faulstich, H. (1996) Identification of contact sites in the actin-thymosin beta 4 complex by distance-dependent thiol cross-linking. *J. Biol. Chem. 271* (3), 1301−1308.

(10) Pardee, J. D., and Spudich, J. A. (1982) Purification of muscle actin. *Methods Enzymol. 85* (Pt B), 164−181.

(11) Paavilainen, V. O., Oksanen, E., Goldman, A., and Lappalainen, P. (2008) Structure of the actin-depolymerizing factor homology domain in complex with actin. *J. Cell Biol. 182* (1), 51−59.

(12) Tripos, Inc. (2006) *Sybyl, Verson 7.3*; Tripos: St. Louis, MO.

(13) Case, D. A.; Darden, T. A.; Cheatham, T. E., III; Simmerling, C. L.; Wang, J.; Duke, R. E.; Luo, R.; Walker, R. C.; Zhang, W.; Merz, K. M.; Roberts, B.; Wang, B.; Hayik, S.; Roitberg, A.; Seabra, G.; Kolossváry, I.; Wong, K. F.; Paesani, F.; Vanicek, J.; Liu, J.; Wu, X.; Brozell, S. R.; Steinbrecher, T.; Gohlke, H.; Cai, Q.; Ye, X.; Wang, J.; Hsieh, M.-J.; Cui, G.; Roe, D. R.; Mathews, D. H.; Seetin, M. G.; Sagui, C.; Babin, V.; Luchko, T.; Gusarov, S.; Kovalenko, A.; Kollman, P. A. (2010) *AMBER*11, University of California, San Francisco, CA.

(14) (a) Cheatham, T. E., Cieplak, P., and Kollman, P. A. (1999) A modified version of the Cornell et al. force field with improved sugar pucker phases and helical repeat. *J. Biomol. Struct. Dyn. 16* (4), 845−862. (b) Hornak, V., Abel, R., Okur, A., Strockbine, B., Roitberg, A., and Simmerling, C. (2006) Comparison of multiple amber force fields and development of improved protein backbone parameters. *Proteins 65* (3), 712−725. (c) Lindorff-Larsen, K., Piana, S., Palmo, K., Maragakis, P., Klepeis, J. L., Dror, R. O., and Shaw, D. E. (2010) Improved side-chain torsion potentials for the Amber ff99SB protein force field. *Proteins 78* (8), 1950−1958.

(15) Onufriev, A., Bashford, D., and Case, D. A. (2004) Exploring protein native states and large-scale conformational changes with a modified generalized born model. *Proteins 55* (2), 383−394.

(16) Humphrey, W., Dalke, A., and Schulten, K. (1996) VMD: visual molecular dynamics. *J. Mol. Graphics 14* (1), 33−38.

(17) Green, N. S., Reisler, E., and Houk, K. N. (2001) Quantitative evaluation of the lengths of homobifunctional protein cross-linking reagents used as molecular rulers. *Protein Sci. 10* (7), 1293−1304.

(18) Hannappel, E.; Huff, T.; Safer, D. (2006) in *Actin Monomer Binding Proteins* (Lappalainen, P., Ed.) pp 61−70, Landes Bioscience/Eurekah.com: Austin, TX.

(19) (a) Chereau, D., Kerff, F., Graceffa, P., Grabarek, Z., Langsetmo, K., and Dominguez, R. (2005) Actin-bound structures of Wiskott-Aldrich syndrome protein (WASP)-homology domain 2 and the implications for filament assembly. *Proc. Natl. Acad. Sci. U. S. A. 102* (46), 16644−16649. (b) Hertzog, M., van Heijenoort, C., Didry, D., Gaudier, M., Coutant, J., Gigant, B., Didelot, G., Preat, T., Knossow, M., Guittet, E., and Carlier, M. F. (2004) The beta-thymosin/WH2 domain; structural basis for the switch from inhibition to promotion of actin assembly. *Cell 117* (5), 611−623.

(20) (a) Tanokura, M. (1983) 1H-NMR study on the tautomerism of the imidazole ring of histidine residues. II. Microenvironments of histidine-12 and histidine-119 of bovine pancreatic ribonuclease A. *Biochim. Biophys. Acta 742* (3), 586−596. (b) Vila, J. A., Arnautova, Y. A., Vorobjev, Y., and Scheraga, H. A. (2011) Assessing the fractions of

tautomeric forms of the imidazole ring of histidine in proteins as a function of pH. *Proc. Natl. Acad. Sci. U. S. A. 108* (14), 5602−5607.
(21) Holmes, K. C., Popp, D., Gebhard, W., and Kabsch, W. (1990) Atomic model of the actin filament. *Nature 347* (6288), 44−49.
(22) Oda, T., Iwasa, M., Aihara, T., Maeda, Y., and Narita, A. (2009) The nature of the globular- to fibrous-actin transition. *Nature 457* (7228), 441−445.
(23) (a) Kabsch, W., Mannherz, H. G., and Suck, D. (1985) Three-dimensional structure of the complex of actin and DNase I at 4.5 A resolution. *EMBO J. 4* (8), 2113−2118. (b) Kabsch, W., Mannherz, H. G., Suck, D., Pai, E. F., and Holmes, K. C. (1990) Atomic structure of the actin:DNase I complex. *Nature 347* (6288), 37−44.
(24) Rubin, B. K., Kater, A. P., and Goldstein, A. L. (2006) Thymosin beta4 sequesters actin in cystic fibrosis sputum and decreases sputum cohesivity in vitro. *Chest 130* (5), 1433−1440.
(25) Reichert, A., Heintz, D., Echner, H., Voelter, W., and Faulstich, H. (1996) The ternary complex of DNase I, actin and thymosin beta4. *FEBS Lett. 387* (2−3), 132−136.
(26) Ballweber, E., Giehl, K., Hannappel, E., Huff, T., Jockusch, B. M., and Mannherz, H. G. (1998) Plant profilin induces actin polymerization from actin: beta-thymosin complexes and competes directly with beta-thymosins and with negative co-operativity with DNase I for binding to actin. *FEBS Lett. 425* (2), 251−255.
(27) Schutt, C. E., Myslik, J. C., Rozycki, M. D., Goonesekere, N. C., and Lindberg, U. (1993) The structure of crystalline profilin-beta-actin. *Nature 365* (6449), 810−816.
(28) Talens, S., Leebeek, F. W., Demmers, J. A., and Rijken, D. C. (2012) Identification of fibrin clot-bound plasma proteins. *PLoS One 7* (8), e41966.
(29) Huff, T., Otto, A. M., Müller, C. S., Meier, M., and Hannappel, E. (2002) Thymosin b_4 is released from human blood platelets and attached by factor XIIIa (transglutaminase) to fibrin and collagen. *FASEB J. 16* (7), 691−696.
(30) Huff, T., Ballweber, E., Humeny, A., Bonk, T., Becker, C., Muller, C. S., Mannherz, H. G., and Hannappel, E. (1999) Thymosin beta(4) serves as a glutaminyl substrate of transglutaminase. Labeling with fluorescent dansylcadaverine does not abolish interaction with G-actin. *FEBS Lett. 464* (1−2), 14−20.
(31) Eligula, L., Chuang, L., Phillips, M. L., Motoki, M., Seguro, K., and Muhlrad, A. (1998) Transglutaminase-induced cross-linking between subdomain 2 of G-actin and the 636−642 lysine-rich loop of myosin subfragment 1. *Biophys. J. 74* (2 Pt 1), 953−963.
(32) Benchaar, S. A., Xie, Y., Phillips, M., Loo, R. R., Galkin, V. E., Orlova, A., Thevis, M., Muhlrad, A., Almo, S. C., Loo, J. A., Egelman, E. H., and Reisler, E. (2007) Mapping the interaction of cofilin with subdomain 2 on actin. *Biochemistry (Moscow) 46* (1), 225−233.
(33) Kamal, J. K., Benchaar, S. A., Takamoto, K., Reisler, E., and Chance, M. R. (2007) Three-dimensional structure of cofilin bound to monomeric actin derived by structural mass spectrometry data. *Proc. Natl. Acad. Sci. U. S. A. 104* (19), 7910−7915.
(34) (a) Czisch, M., Schleicher, M., Horger, S., Voelter, W., and Holak, T. A. (1993) Conformation of thymosin beta 4 in water determined by NMR spectroscopy. *Eur. J. Biochem. 218* (2), 335−344. (b) Simenel, C., Van Troys, M., Vandekerckhove, J., Ampe, C., and Delepierre, M. (2000) Structural requirements for thymosin beta4 in its contact with actin. An NMR-analysis of thymosin beta4 mutants in solution and correlation with their biological activity. *Eur. J. Biochem. 267* (12), 3530−3538.
(35) De La Cruz, E. M., Ostap, E. M., Brundage, R. A., Reddy, K. S., Sweeney, H. L., and Safer, D. (2000) Thymosin-beta(4) changes the conformation and dynamics of actin monomers. *Biophys. J. 78* (5), 2516−2527.